J|A|C|S
COMMUNICATIONS

Published on Web 05/17/2007

Ultralong Nanobelts Self-Assembled from an Asymmetric Perylene Tetracarboxylic Diimide

Yanke Che, Aniket Datar, Kaushik Balakrishnan, and Ling Zang*

Department of Chemistry and Biochemistry, Southern Illinois University, Carbondale, Illinois 62901

Received March 18, 2007; E-mail: lzang@chem.siu.edu

One-dimensional (1D) self-assembly of planar aromatic (semiconductor) molecules into well-defined nanowires or nanobelts has gained increasing interest[1] since such an approach may extend the optoelectronic properties and applications intrinsic to organic semiconductors from film-based materials into the size ranges and architectures that have never before been achieved. Among the small number of molecules successfully explored in such 1D self-assembly,[2−8] symmetric molecules modified with all identical side chains represent the majority of building block candidates.[2−6] In contrast, there have been much less asymmetric molecules employed in the fabrication of well-defined nanowires or nanobelts,[1b,2,8] although asymmetric molecules may provide more options and adaptability for the surface modification to approach optimized sensing sensitivity and selectivity for the nanomaterials thus fabricated.[8b]

In this Communication, we report for the first time the fabrication of ultralong nanobelts (>0.3 mm) from an asymmetric perylene tetracarboxylic diimide (PTCDI) molecule as shown in Chart 1. PTCDIs represent a unique class of molecules that demonstrate extremely high thermal and photostability and have been employed in a wide variety of film-based optoelectronic devices.[3,9] While well-defined nanowires have recently been fabricated from various symmetric PTCDIs,[3,5,10] which possess identical linear side chains at the two imide positions, there is no such 1D self-assembly reported on the asymmetric PTCDIs. The new self-assembly approach reported herein on the asymmetric PTCDI will open broader options for both molecular design and engineering to improve the fabrication of 1D nanomaterials. Moreover, the *millimeter* long nanobelt fabricated in this study will enable more expedient construction of integrated nanoelectronic devices, for which deposition of a wire across multiple parallel electrodes is usually demanded.[11]

The polyoxyethylene side-chain attachment makes molecule **1** highly soluble in hydrophilic solvents such as ethanol. Taking advantage of the miscibility between alcohol and water, the solubility (or self-assembly) of the molecule can feasibly be controlled by adjusting the volume ratio of water and alcohol (detailed in the Supporting Information). Upon increasing the water component, the increase in solvent polarity will force solvophobic association between the alkyl side chains, in a similar manner of 1D self-assembly of surfactants and other amphiphilic molecules.[12−14] Such hydrophobic interdigitation will bring the molecules in proximity where the $\pi-\pi$ interaction dominates the molecular packing configuration. The $\pi-\pi$ molecular stacking is likely facilitated by the stretching-out conformation of the polyoxyethylene side chain, which is favored in hydrophilic solvent.[8a] Indeed, ultralong nanobelt structure was obtained from the self-assembly of compound **1** in water/ethanol solution at an appropriate volume ratio, ca. 1:1.

As demonstrated by the large-area SEM imaging shown in Figure 1A, ultralong fibril structure was formed through a slow 1D crystalline growing process, typically over 5 days, in a 1:1 water/ethanol solvent (Supporting Information). Such a slow crystallization process allows for more organized molecular stacking and more extended growth along the fibril long axis. Most of the fibers are more than 0.3 mm in length, and some of them even reach ca. 0.5 mm (Figure S4). AFM imaging over a single fiber revealed the belt-like morphology, with a width-to-thickness aspect ratio of ca. 10:1 (Figure S6). Such nanobelt conformation was also demonstrated by small-area SEM imaging (Figure S5), where twisted nanobelts are clearly unveiled, showing the same width-to-thickness aspect ratio as that imaged by AFM. The extended 1D self-assembly is likely dominated by the strong $\pi-\pi$ interaction between the PTCDI scaffolds, as indicated by the X-ray diffraction (Figure S8), for which the typical $\pi-\pi$ stacking peak (with *d*-spacing = 3.57 Å) was observed. The first and third diffraction peaks (*d*-spacing = 38.2 and 12.6 Å) are assigned to the edge-to-edge distances between two adjacent PTCDI molecules at the longitudinal and transverse directions, while the second peak is likely due to the secondary diffraction of the longitudinal molecular arrangement since the *d*-spacing is about half of the value of the first peak.

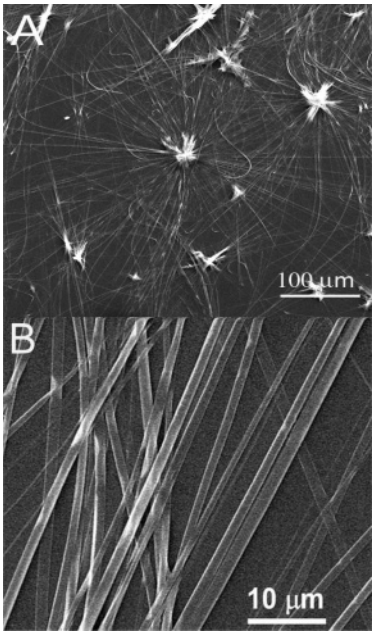

Figure 1. (A) A large-area SEM image showing the growth of long nanobelts from the central seeding particulate aggregates. (B) A zoom-in image showing the belt morphology and uniform size of the nanobelts.

Chart 1

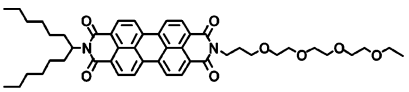

(1)

10.1021/ja071903w CCC: $37.00

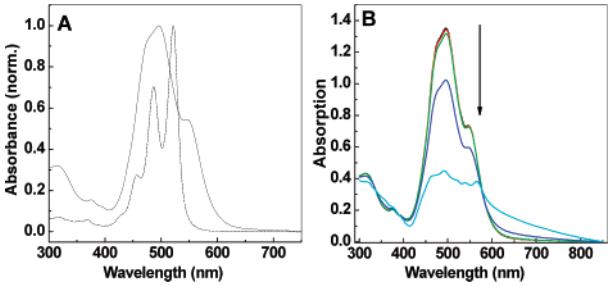

Figure 2. (A) UV−vis absorption spectra of **1** (0.6 mM) molecularly dissolved in ethanol (dotted line) and in the aggregate state dispersed in 1:1 water/ethanol (solid line). (B) Absorption spectra of the aggregate shown in (A) at different aging times: 0, 5, 24, 48, 72 h. A 2 mm cell was used.

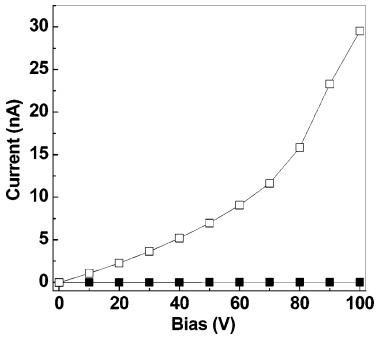

Figure 3. *I*−*V* curves measured on a single nanobelt deposited across a pair of gold electrodes separated by 80 μm: (□) in saturated vapor of hydrazine (140 ppm), (■) in air. Long nanobelt enables expedient deposition across the large electrode gap.

Considering the self-assembling mechanism hypothesized above, if the solvent polarity is too high (i.e., with more volume of water), the molecular aggregation would become too fast due to the stronger solvophobic association between the hexylheptyl chains, thereby leading to formation of more seeding particles and leaving no free molecules available for the later stage growth of the nanobelt. Indeed, when increasing the volume ratio of water from 1:1 to 5:1, only particulate aggregates and some very short nanofibers were formed from the self-assembly (Figure S7).

The self-assembling of **1** was monitored by the absorption spectral measurement. Upon addition of water to the ethanol solution of **1**, a new absorption band emerged at ca. 550 nm (Figure 2), indicative of the $\pi-\pi$ stacking state of the PTCDI molecules.[3,5] Moreover, with the aging time, the absorption below 550 nm (corresponding to individual molecules) was gradually decreased, while the absorption at longer wavelength (due to the extended aggregate state) became enhanced. An approximate isobestic point at 581 nm indicates the stoichiometric conversion from the initially formed small aggregates (nucleation seeds) to the long nanobelt structures. The relative stronger absorption at longer wavelengths is consistent with the extended molecular stacking within the long nanobelts, for which the electronic transition is primarily determined by the collective interaction between the large number of cofacially stacked molecules.

The extended $\pi-\pi$ stacking along the long axis of the nanobelt would enable efficient long-range charge migration due to the effective intermolecular π-electron delocalization[15] and thus allow increasing the electrical conductivity of the nanobelt through external charge doping. Figure 3 shows the current−voltage (*I*−*V*) measurement of a single nanobelt in the presence and absence of hydrazine vapor, a strong reducing reagent that is capable of donating an electron into the nanobelt through ground-state redox reaction (hydrazine, E°_{ox} +0.43 V, vs SCE; PTCDI E°_{red} −0.59 V, vs SCE). Under an applied bias, the doped electrons will rapidly migrate along the long axis of the nanobelt, due to the long-range band-like π-electron delocalization along the nanobelt, leading to significant enhancement in current. Indeed, over 3 orders of magnitude increase in current was observed for the nanobelt upon exposure to the saturated vapor of hydrazine. Such high current modulation, along with the ultralong length, will make the nanobelts ideal building blocks in optoelectronic nanodevices.

In summary, millimeter long nanobelts have been fabricated from an asymmetric PTCDI molecule through a seeded self-assembling method. The long length of nanobelts facilitates the construction of two-electrode devices employing the nanobelt as channel material; the long-range $\pi-\pi$ molecular stacking allows for efficient conductivity modulation through surface doping. A combination of these two characters will enable broad optoelectronic applications with these long nanobelts.

Acknowledgment. This work was supported by NSF (CMMI 0638571), ACS-PRF (45732-G10), and NSFC (20520120221). We thank Dr. Tiede for help with the XRD measurement.

Supporting Information Available: Synthesis, *I*−*V*, spectroscopy, and microscopy measurements. This material is available free of charge via the Internet at http://pubs.acs.org.

References

(1) (a) Hoeben, F. J. M.; Jonkheijm, P.; Meijer, E. W.; Schenning, A. P. H. J. *Chem. Rev.* **2005**, *105*, 1491−1546. (b) Grimsdale, A. C.; Müllen, K. *Angew Chem., Int. Ed.* **2005**, *44*, 5592.

(2) Xiao, S.; Tang, J.; Beetz, T.; Guo, X.; Tremblay, N.; Siegrist, T.; Zhu, Y.; Steigerwald, M.; Nuckolls, C. *J. Am. Chem. Soc.* **2006**, *128*, 10700.

(3) Wurthner, F. *Chem. Commun.* **2004**, *14*, 1564.

(4) Shirakawa, W.; Fujita, N.; Shinkai, S. *J. Am. Chem. Soc.* **2005**, *127*, 4164.

(5) (a) Balakrishnan, K.; Datar, A.; Oitker, R.; Chen, H.; Zuo, J.; Zang, L. *J. Am. Chem. Soc.* **2005**, *127*, 10496. (b) Datar, A.; Balakrishnan, K.; Yang, X.; Zuo, X.; Huang, J.; Oitker, R.; Yen, M.; Zhao, J.; Tiede, D. M.; Zang, L. *J. Phys. Chem. B* **2006**, *110*, 12327. (c) Balakrishnan, K.; Datar, A.; Naddo, T.; Huang, J.; Oitker, R.; Yen, M.; Zhao. J.; Zang, L. *J. Am. Chem. Soc.* **2006**, *128*, 6576.

(6) Balakrishnan, K.; Datar, A.; Zhang, W.; Yang, X.; Naddo, T.; Huang, J.; Zuo, J.; Yen, M.; Moore, J. S.; Zang, L. *J. Am. Chem. Soc.* **2006**, *128*, 6576.

(7) Briseno, A. L.; Mannsfeld, S. C. B.; Lu, X.; Xiong, Y.; Jenekhe, S. A.; Bao, Z.; Xia, Y. *Nano Lett.* **2007**, *7*, 668.

(8) (a) Yamamoto, Y.; Fukushima, T.; Suna, Y.; Ishii, N.; Saeki, A.; Seki, S.; Tagawa, S.; Taniguchi, M.; Kawai, T.; Aida, T. *Science* **2006**, *314*, 1761. (b) Hill, J. P.; Jin, W.; Kosaka, A.; Fukushima, T.; Ichihara, H.; Shimomura, T.; Ito, K.; Hashizume, T.; Ishii, N.; Aida, T. *Science* **2004**, *304*, 1481.

(9) (a) Newman, C. R.; Frisbie, C. D.; da Silva Filho, D. A.; Bredas, J.-L.; Ewbank, P. C.; Mann, K. R. *Chem. Mater.* **2004**, *16*, 4436. (b) Law, K.-Y. *Chem. Rev.* **1993**, *93*, 449. (c) Jones, B. A.; Ahrens, M. J.; Yoon, M.-H.; Facchetti, A.; Marks, T. J.; Wasielewski, M. R. *Angew. Chem., Int. Ed.* **2004**, *43*, 6363. (d) Schmidt-Mende, L.; Fechtenkotter, A.; Mullen, K.; Moons, E.; Friend, R. H.; MacKenzie, J. D. *Science* **2001**, *293*, 1119.

(10) Palermo, V.; Liscio, A.; Gentilini, D.; Nolde, F.; Müllen, K.; Samori, P. *Small* **2007**, *3*, 161.

(11) (a) Kim, W.; Choi, C. H.; Shim, M.; Li, Y.; Wang, D.; Dai, H. *Nano Lett.* **2002**, *2*, 703. (b) Xia, Y.; Yang, P.; Sun, Y.; Wu, Y.; Mayers, B.; Gates, B.; Yin, Y.; Kim, F.; Yan, H. *Adv. Mater.* **2003**, *15*, 353.

(12) Paramonov, S. E.; Jun, H.; Hartgerink, J. D. *J. Am. Chem. Soc.* **2006**, *128*, 7291−7298.

(13) (a) Hartgerink, J. D.; Beniash, E.; Stupp, S. I. *Science* **2001**, *294*, 1684. (b) Genson, K. L.; Holzmueller, J.; Ornatska, M.; Yoo, Y.-S.; Par, M.-H.; Lee, M.; Tsukruk, V. V. *Nano Lett.* **2006**, *6*, 435. (c) Zubarev, E. R.; Sone, E. D.; Stupp, S. I. *Chem.−Eur. J.* **2006**, *12*, 7313−7327.

(14) Beck, J. S.; Vartuli, J. C.; Roth, W. J.; Leonowicz, M. E.; Kresge, C. T.; Schmitt, K. D.; Chu, C. T.-W.; Olson, D. H.; Sheppard, E. W.; McCullen, S. B.; Higgins, J. B.; Schlenke, J. L. *J. Am. Chem. Soc.* **1992**, *114*, 10834.

(15) (a) Lemaur, V.; da Silva Filho, D. A.; Coropceanu, V.; Lehmann, M.; Geerts, Y.; Piris, J.; Debije, M. G.; van de Craats, A. M.; Senthilkumar, K.; Siebbeles, L. D. A.; Warman, J. M.; Bredas, J.-L.; Cornil, J. *J. Am. Chem. Soc.* **2004**, *126*, 3271. (b) Crispin, X.; Cornil, J.; Friedlein, R.; Okudaira, K. K.; Lemaur, V.; Crispin, A.; Kestemont, G.; Lehmann, M.; Fahlman, M.; Lazzaroni, R.; Geerts, Y.; Wendin, G.; Ueno, N.; Bredas, J.-L.; Salaneck, W. R. *J. Am. Chem. Soc.* **2004**, *126*, 11889.

JA071903W